High order sliding mode control of active and reactive powers for DFIG based Wind turbine

Ouassima El qouarti,[1,*] *Ahmed* Essadki,[1] and *Tamou* Nasser[2]

[1]ERERA, Research Center in Sciences and Technologies of Engineering and Health (STIS) Ecole Nationale Supérieure d'Arts et Métiers (ENSAM), Mohammed V University in Rabat, Morocco
[2] Ecole Nationale Supérieure d'Informatique et d'Analyse des Systèmes (ENSIAS), Mohammed V University in Rabat, Morocco

Abstract. Grid connected wind turbines are considered as a wise alternative to conventional energy sources; not only they are used to produce energy, but they have been recently operated in order to provide grid ancillary services such as stability and frequency control. In this paper we are going to deal with the famous doubly fed induction generator (DFIG) based Wind Energy Conversion Systems (WECS) for its variable speed operation and excellent power quality. The purpose of this study is to apply a High Order Sliding Mode Control (HOSMC) based on vector control and to compare the results with the first order sliding mode control (FOSMC) in order to evaluate the performances of stability and chattering elimination under normal conditions. Simulation results show the superiority of the SOSMC over the FOSMC in terms of robustness and chattering elimination. Keywords: DFIG, Vector Control, High order sliding mode, Super-twisting, WECS.

1 Introduction

Nowadays, almost everywhere in the world, and more particularly in Morocco, Renewable Energy (RnE) and especially wind energy are strongly called to be integrated into the electrical network to support the increasing demand for electrical energy while minimizing the costs of production. The total wind power capacity installed in the world, at the end of 2018, has reached 591 GW [1].

We focus in this study on wind energy and particularly horizontal axis variable speed Wind Turbine (WT) with partial-scale power converter based on Doubly Fed Indiction Generator (DFIG). The diagram of the studied wind turbine can be found at [2]. DFIG is the most used technique for wind energy production due to its ability to work effectively under variable speed conditions, the possibility to control active and reactive power and the use of converters of reduced size and cost since they transmit a reduced rotor power [2] [3]. SMC is one of the non-linear promising DFIG control techniques present in literature. It has simple structure, allows DC voltage maintenance and direct control of power, furthermore it has proven robustness against uncertainties and external disturbances. All these features and others have made it a more robust control choice [4]. Based SMC techniques as well as its succeeding variants (FOSMC, ST-HOSMC, etc.) have proven efficiency and high performances addressing issues related to uncertainties and system disturbances. In this paper we are going to simulate FOSMC and SOSMC based on Stator Field Oriented (SFO) vector control for DFIG. This study aims to highlight the performances of these two control techniques in terms of robustness and chattering attenuation.

The structure of the present paper is: A general introduction in the first part. The adopted power control strategy is shown in the second part. The third part is dedicated to SMC and High order sliding mode control strategies. In the fourth part are shown the Simulation results and analysis. A conclusion is set towards the end.

2 Power control strategy

In this study, we are going to choose the classical vector control based on SFO power control strategy. [5] et [6]. The stator field is chosen to be aligned with d-axis.

* Corresponding author: elqouarti.ouassima@gmail.com

Figure 1 shows the vector control simplified block diagram that will be regulated. Active and reactive powers are as in (1), (2). Rotor voltages are expressed in (3), (4).

$$P_s = -V_s \frac{L_m}{L_s} I_{qr} \tag{1}$$

$$Q_s = V_s \frac{\Phi_s}{L_s} - V_s \frac{L_m}{L_s} I_{dr} \tag{2}$$

$$V_{dr} = \left(R_r + s\left(L_r - \frac{L_m^2}{L_s}\right)\right) I_{dr} - g\,\omega_s \left(L_r - \frac{L_m^2}{L_s}\right) I_{qr} \tag{3}$$

$$V_{qr} = \left(R_r + s\left(L_r - \frac{L_m^2}{L_s}\right)\right) I_{qr} + g\,\omega_s \left(L_r - \frac{L_m^2}{L_s}\right) I_{dr} + g\frac{L_m V_s}{L_s} \tag{4}$$

Where : g is the ratio between wr and ws.

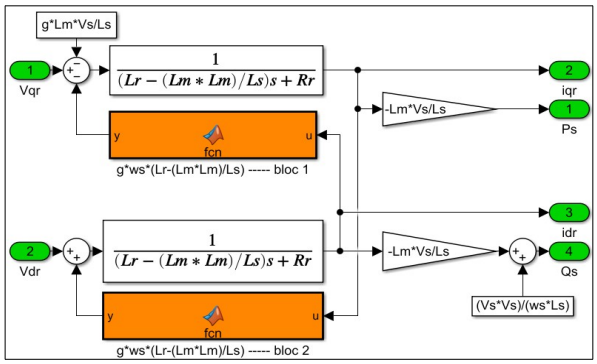

Fig. 1. Vector control simplified block diagram.

3 High order sliding mode control

3.1 First order sliding mode control

3.1.1 Definitions

SMC is a variable structure control that has been widely used to control non-linear systems [7]. It allows the control despite of uncertainties and disturbances [7], [8]

SMC design depends on 3 components: [8], [9]

- Choice of the switching (sliding) surface

Following up, is a representation of a non linear system:

$$\dot{Z} = h(Z,t) + k(Z,t)\,v(Z,t); Z \in R^n, v \in R \tag{5}$$

$$S(Z) = \left(\frac{d}{dt} + a\right)^{m-1} e(Z) \tag{6}$$

$$er(Z) = Z^d - Z \tag{7}$$

The two functions h and k are continuous, non-linear, uncertain and supposed bounded.

er: the error on the signal we want adjusting; Zd: signal reference; Z: the state variable of the control signal; a: a positive coefficient; m: the order of the system. [9]

- The convergence condition: Stability analysis of the used control is verified via the Lyapunov function [8].

$$S(Z)\dot{S}(Z) \leqslant 0 \tag{8}$$

- The control law, which is defined as follow :

$$v = v^{eq} + v^n \tag{9}$$

v is the control variable; v^{eq} is the equivalent control term; v^n is the switching control term.

Generally, the expression of the switching term is as follow:

$$v^n = b\,sign(S) \tag{10}$$

b : a positive constant; v^n : the discontinuous command.

3.1.2 DFIG Rotor side control based SMC

- Choice of the switching surface: In this part we aim to control active and reactive powers. Their switching surfaces are mentioned in [9] as (11) and (12) :

$$S(P) = P_s^{ref} - P_s \tag{11}$$

$$S(Q) = Q_s^{ref} - Q_s \tag{12}$$

$$\dot{S}(P) = \dot{P_s^{ref}} + V_s \frac{L_m}{L_s L_r \sigma}\left(\left(V_{qr}^{eq} + V_{qr}^n\right) - R_r I_{qr}\right) \tag{13}$$

$$\dot{S}(Q) = \dot{Q_s^{ref}} + V_s \frac{L_m}{L_s L_r \sigma}\left(\left(V_{dr}^{eq} + V_{dr}^n\right) - R_r I_{dr}\right) \tag{14}$$

$$\sigma = 1 - \frac{L_m^2}{L_s L_r} \tag{15}$$

We choose rotor voltages as the control signals (v). The equivalent control terms are as in equations (16) and (17):

$$V_{qr}^{eq} = -\dot{P_s^{ref}} \frac{\sigma L_s L_r}{V_s L_m} + R_r I_{qr} + (\sigma L_r g\,\omega_s) I_{dr} + \frac{g L_m V_s}{L_s} \tag{16}$$

$$V_{dr}^{eq} = -\dot{Q_s^{ref}} \frac{\sigma L_s L_r}{V_s L_m} + R_r I_{dr} - (\sigma L_r g\,\omega_s) I_{qr} \tag{17}$$

- The convergence condition in equation (8) is verified for P and Q. [9]

- Control law: The switching terms are expressed as in [10]:

$$V_{qr}^n = -K_1\,sign(S(P)) \tag{18}$$

$$V_{dr}^n = -K_2\,sign(S(Q)) \tag{19}$$

Constants K_1 and K_2 must be positive to verify the system stability.

Figure 2 presents the block diagram of the FOSMC. Later, in the simulation, we will take: $Kv_{qr} = -K_1$ and $K_{Vdr} = -K_2$.

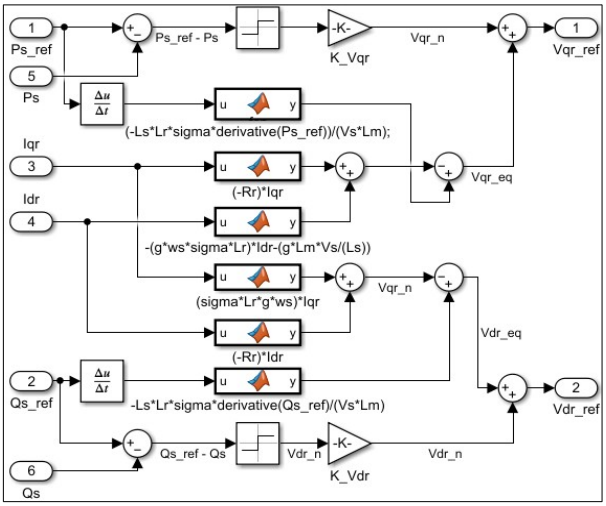

Fig. 2. Block diagram of FOSMC.

3.2 Second order sliding mode control

3.2.1 Definitions

SOSMC algorithms provide, in addition to properties granted by the conventional sliding mode control, the possibility to help mitigate the chattering in the system [8]. Many SOSMC algorithms were studied in the literature, [7]. This publication presents the ST algorithm. This algorithm is made up of a discontinuous part v_2 and a continuous part v_1:

$$v = v_1(t) + v_2(t) \tag{20}$$

Based on [8], we write the simplified form of the algorithm as :

$$v = -\lambda |S|^{\mu} sign(S) + v_1 \tag{21}$$

$$\dot{v}_1 = -\beta \, sign(S) \tag{22}$$

λ, μ and β satisfy the following conditions :

$$\beta > \frac{B_0}{K} \quad ; \quad 0 < \mu < 0.5 \tag{23}$$

$$\lambda^2 > \frac{4 B_0 K'(\beta + B_0)}{K^2 K(\beta - B_0)} \quad if \;\; \mu = 0.5 \tag{24}$$

B_0, K and K' are positive constants.

3.2.2 DFIG Rotor side control

Based on [8][10], the ST active and reactive power controllers are designed, respectively, as in (25) and (26) :

$$V_{qr} = -\lambda_1 |S|^{\mu} signS(P_s) - \int \alpha_1 signS(P_s) \tag{25}$$

$$V_{dr} = -\lambda_2 |S|^{\mu} signS(Q_s) - \int \alpha_2 signS(Q_s) \tag{26}$$

α_1 and α_2 verify the stability conditions in (23), (24).

Figure 3 presents the block diagram of the SOSMC.

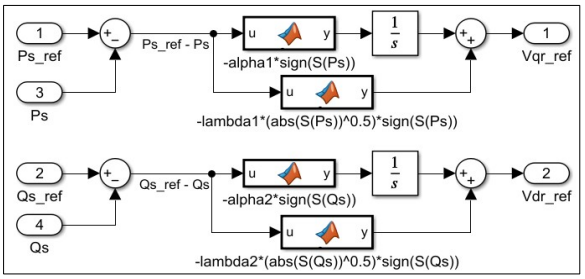

Fig. 3. Block diagram of SOSMC.

4 Simulation results and analysis

Simulations were conducted in Matlab/Simulink for a 7.5KW DFIG. The rotor surface of the WT is 18,85m². The wind speed was fixed at 10m/s, and the pitch angle β at 2. Data related to this study are presented in Table 2. Figure 4, shows the signal references used, respectively for active and reactive powers. This signal allows us to demonstrate the performances of the two controllers and their ability to track the reference. In Figure 5 and Figure 6 are plotted, respectively, the active and reactive power graphs resulting from each control. Both controls are compared according to their contribution in power quality enhancement, eventually by their capacity to attenuate the chattering phenomenon.

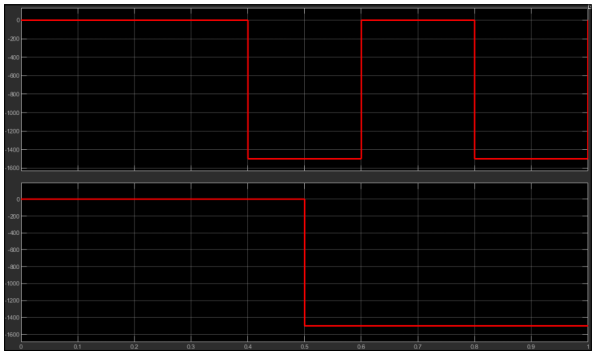

Fig. 4. Signal references of active and reactive powers.

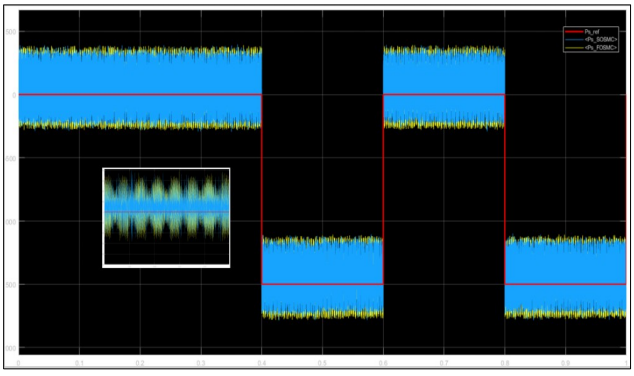

Fig. 5. Stator active power signals.

Graphs show that the two controls are able to track the reference values, in addition the SOSMC is more efficient in term of chattering elimination and thus, it guarantees an improved power quality to be injected into the grid.

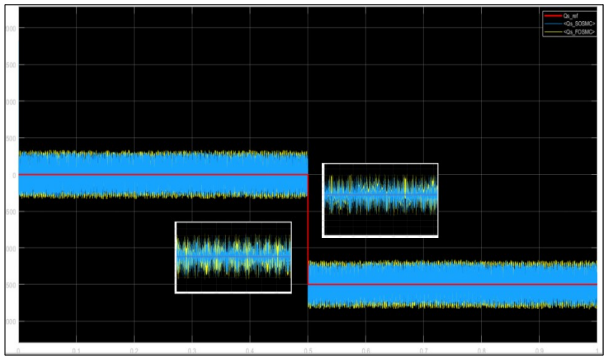

Fig. 6. Stator reactive power signals. Yellow : Qs_FOSMC, Blue : Qs_SOSMC, Red : Qs_ref.

Table 1. Nomenclature.

Parameter	Description
Tem	Electromagnetic torque of the generator
s	Laplace operator
Φqs, Φds	Stator dq fluxes
Φqr, Φd	Rotor dq fluxes
Iqs, Ids	Stator dq currents
Iqr, Idr	Rotor dq currents
p	Number of pole pairs
Lm	Stator mutual inductance
Ls, Lr	Stator and rotor inductace
Rs, Rr	Stator and rotor resistance
ωs, ωr	Stator, rotor angular speed
Vqs, Vds	Stator dq voltages
Vqr, Vd	Rotor dq voltages
g	Slip of the DFIG
f, J	Friction coefficient, The moment of inertia

Table 2. System characteristics.

Parameter	Value
DFIG parameters	
Vs	220 (V)
p	2
Ls	84*10^(-3) (H)
Lr	81*10^(-3) (H)
Lm	78*10^(-3) (H)
Rr	0.62 (Ω)
Rs	0.455 (Ω)
J	0.3125 (Kg.m²)
f	6.73*10^(-3) (N.m)
Vdc	300 (V)
Control design parameters	
alpha1, alpha2	0.5
lambda1 lambda2	2
K_Vqr, K_Vdr	-90000

5 Conclusion and perspectives

In this paper we studied the power control of a DFIG for a variable speed wind turbine. The control strategy has been about applying two different sliding mode controls (FOSMC, SOSMC) on stator active and reactive powers, and to compare their performances in tracking a predefined reference functions. A vector control based SFO was adopted first, in order to simplify the study.

The results support the hypothesis and thus the SOSMC based on ST algorithm showed better responses and robustness, in addition to its efficiency in reducing the chattering phenomenon.

Future works will be focused on applying a third order sliding mode observer to go further in developing techniques useful for the electricity production based wind turbine industry. The aim will be also to respond to the necessity of integrating the electrical grid and optimizing robustness and stability issues.

References

1. GWEC. 51.3 GW of global wind energy capacity installed in 2018. https://www.evwind.es/. last accessed 2021.
2. H. Elouatouat, A. Essadki: *Intelligent control for DFIG-based wind energy conversion system using optimization algorithms. International Conference on Digital Technologies and Applications, ICDTA21.* https://www.youtube.com, last accessed 2021.
3. I. Idrissi: *Contribution au Diagnotic des Défauts de la Machine Asynchrone Doublement Alimentée de l'Eolienne à Vitesse Variable. Thesis. Université Sidi Mohamed Ben Abdellah, Maroc et Université de Rouen Normandie* (2019).
4. I. Sami, S. Ullah, N. Ullah, J. Ro: *Sensorless fractional order composite sliding mode control design for wind generation system. ISA Transactions*, vol. **111**, pp. 275–289 (2021).

5. S. Mensou, A. Essadki, T. Nasser, B. B. Idrissi, L. Ben Tarla: *Dspace DS1104 implementation of a robust nonlinear controller applied for DFIG driven by wind turbine. Renewable Energy*, vol. **147**, pp. 1759–1771 (2020).
6. Y. Dbaghi, S. Farhat, M. Mediouni, H. Essakhi, A. Elmoudden: *High order sliding mode Power control of doubly fed induction generator based on wind turbine. International Conference on Digital Technologies and Applications, ICDTA21*. https://www.youtube.com, last accessed 2021/6/15.
7. F. Mazouz: *Contrôle des puissances active et réactive dans les aérogénérateurs doubles alimentés. Thesis. Université Batna 2 - Mostefa Ben Boulaïd Faculté de Technologie Département de l'Electrotechnique, Algérie.*
8. B. Kelkoul, A. Boumediene: *Stability analysis and study between classical sliding mode control (SMC) and super twisting algorithm (STA) for doubly fed induction generator (DFIG) under wind turbine. Energy*, vol. **214**. *Elsevier Ltd* (2021).
9. M. Allam, Y. Djeriri, H. Mesai Ahmed, I. Dehiba: *Sliding mode control of a doubly fed induction generator for wind energy conversion systems. International Symposium On Technology Sustainable Industry Development, ISTSID'19, Algeria.* (2019).
10. Y. Djeriri: *Robust second order sliding mode control of doubly-fed induction generator for wind energy conversion system. Acta Electrotechnica et Informatica*, vol. **20**, no. 3, pp. 30–38 (2020).